

Supplementary Information

For

A Tunable Temperature-Responsive and Tough Platform for Controlled Drug Delivery

Shuting Gao¹, Aying Zhou¹, Bin Cao¹, Jing Wang², Fanghua Li¹, Guosheng Tang¹, Zhicheng Jiang¹, Anquan Yang², Ranhua Xiong^{3*}, Jiandu Lei^{4*}, Chaobo Huang^{1,5*}

¹College of Chemical Engineering, Jiangsu Co-Innovation Center of Efficient Processing and Utilization of Forest Resources, Nanjing Forestry University, Nanjing, 210037, P. R. China

²OSM Biological co., Ltd, Deqing, 313200, P.R. China

³Lab General Biochemistry & Physical Pharmacy, Department of Pharmaceutics, Ghent University, 9000, Belgium

⁴Beijing Key Laboratory of Lignocellulosic Chemistry, and MOE Engineering Research Center of Forestry Biomass Materials and Bioenergy, Beijing Forestry University, Beijing, 100083, P. R. China

⁵Joint Laboratory of Advanced Biomedical Technology (NFU-UGent), Laboratory of Biopolymer based Functional Materials, Nanjing Forestry University, Nanjing, 210037, P. R. China

Email: huangchaobo@njfu.edu.cn

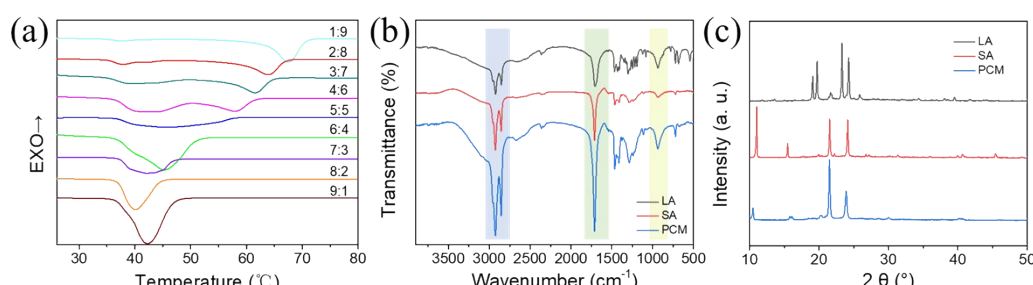


Fig. S1. Characterization of PCM. (a) DSC thermograms for the binary eutectic mixture of LA and SA.

(b) FT-IR spectra and (c) XRD patterns of PCM.

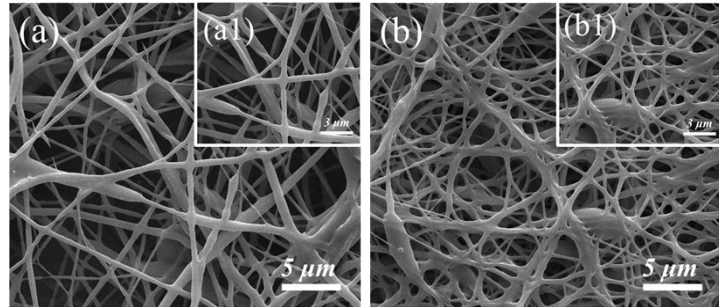


Fig. S2. Characterization of the morphology of the fibers. SEM graphs of (a) Pure PCL fibers and (b) Pure PU fibers.

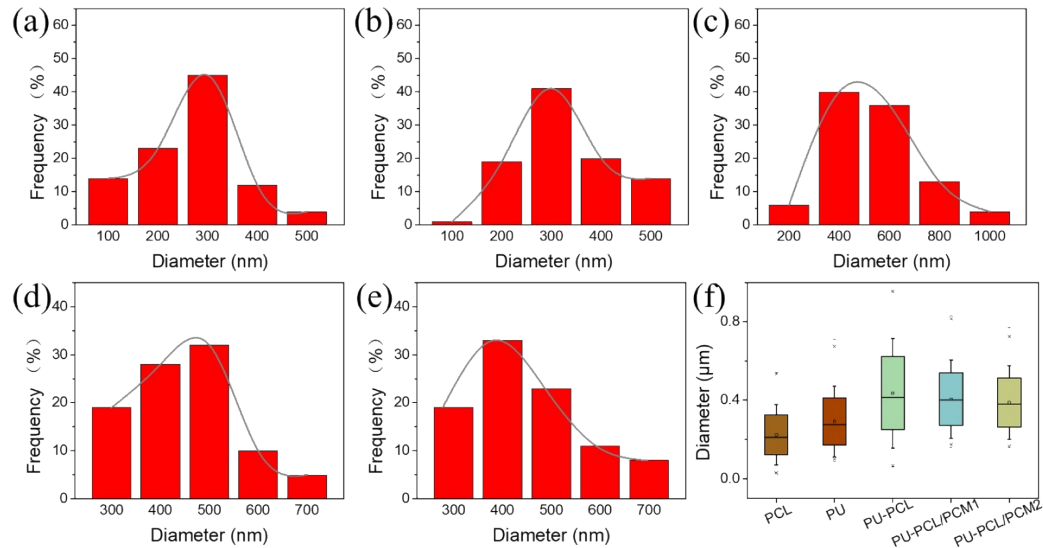


Fig. S3. Fiber diameter histograms of (a) Pure PCL fibrous membranes, (b) Pure PU fibrous membranes, (c) PU-PCL coaxial fibrous membranes, (d) PU-PCL/PCM1 coaxial fibrous membranes ($f_{PCM}=0.05$) and (e) PU-PCL/PCM2 coaxial fibrous membranes ($f_{PCM}=0.1$). (f) Box-plot for diameter (distribution) of the different fibrous membranes.

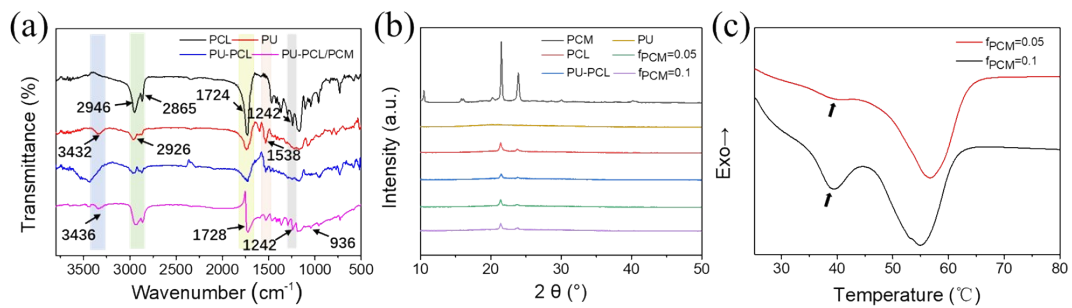


Fig. S4. Characterization of fibers. (a) FT-IR spectra and (b) XRD patterns of fibers. (c) DSC thermograms for the PU-PCL/PCM core-shell fibers of $f_{PCM}=0.05$ and 0.1.

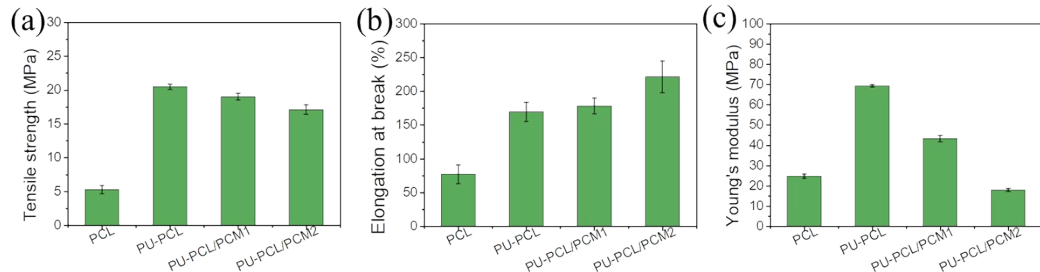


Fig. S5. Mechanical property of fibers. (a) Tensile strength, (b) Elongation at break and (c) Young's modulus of different fibrous membranes.

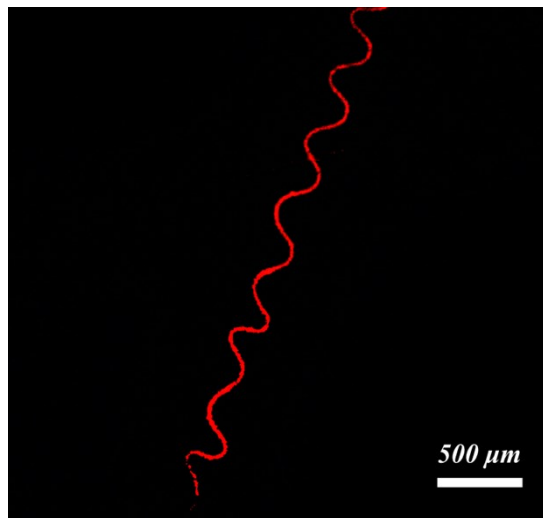


Figure S6. Fluorescence microscopy on Rhodamine B-loaded PU-PCL/PCM1 coaxial fiber.

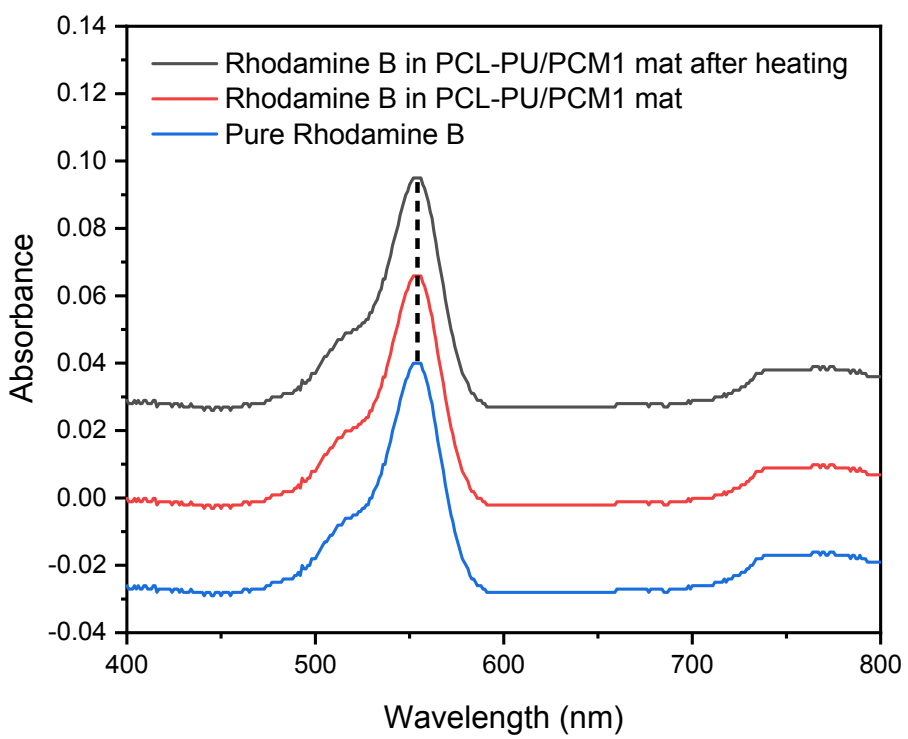


Figure S7. UV-VIS spectra of free Rhodamine B and released media of PU-PCL/PCM1.

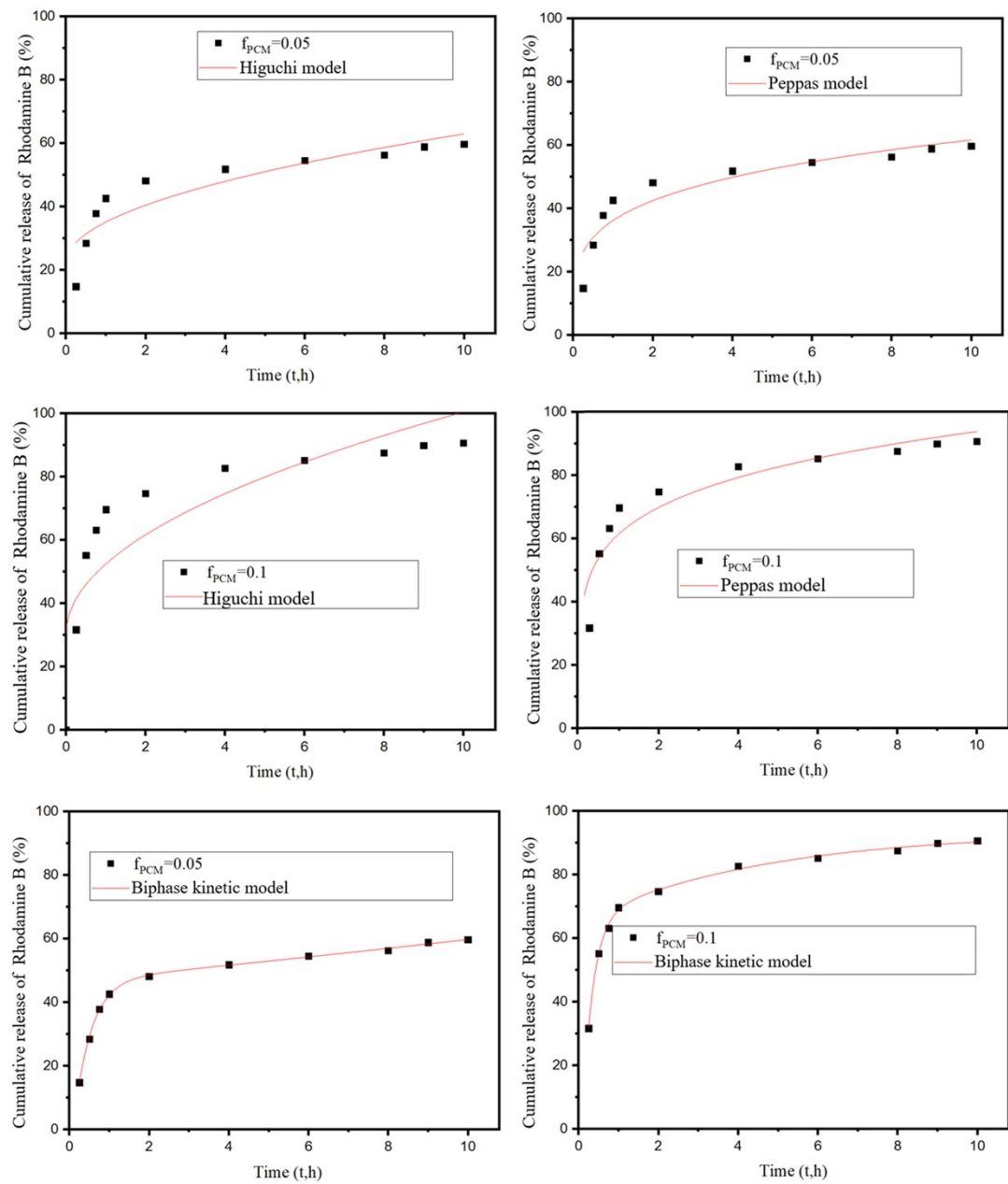


Figure S8. Fitted curves for release kinetic models of PU-PCL/PCM1 ($f_{PCM}=0.05$) and PU-PCL/PCM2 ($f_{PCM}=0.1$)

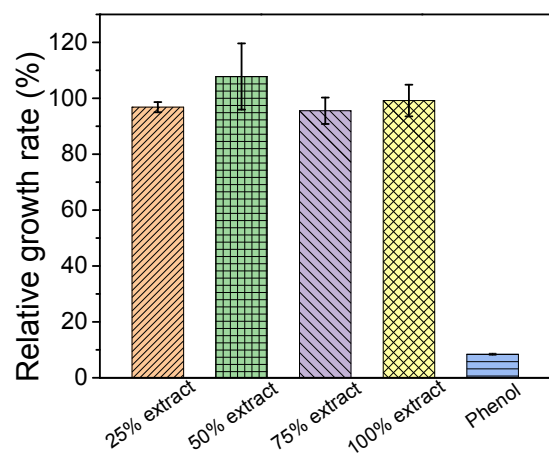


Fig. S9. L929 cell viability quantified by MTT assay. The cells were treated with extract of PU-PCL/PCM fiber membranes.

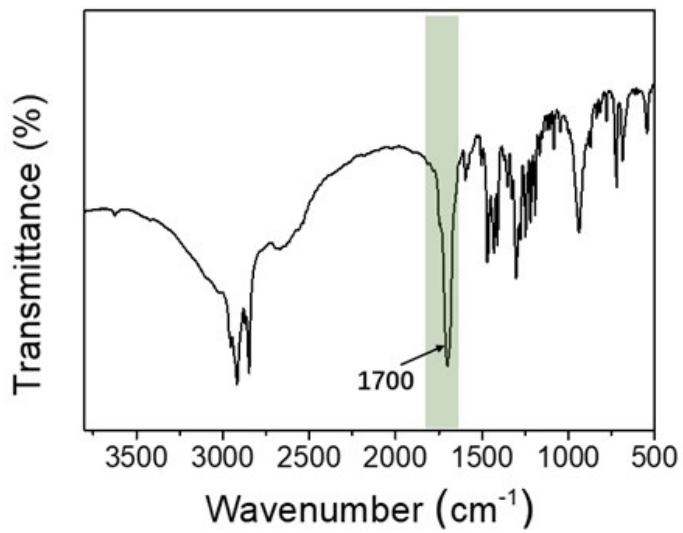


Figure S10. FT-IR spectra of HCPT loaded PU-PCL/PCM1 fiber.

Table S1. Mechanical Properties of the Different Fibers^a

^a Each sample was evaluated for three times. The mean values and the corresponding standard deviations are displayed.

Sample	A	α	B	β	R^2
PU-PCL/PCM1	0.5785 ± 0.0021	-2.3159 ± 0.1819	0.7002 ± 0.0031	-0.0171 ± 0.0068	0.99865
PU-PCL/PCM2	0.2813 ± 0.0019	-0.2188 ± 0.0661	0.9086 ± 0.0083	-3.8156 ± 0.5184	0.99837

Table S2. Specific fitting parameters of Biexponential and Biphase equations

Fibers	Tensile strength (MPa)	Elongation at break (%)	Young's modulus (MPa)
PCL	5.3 ± 0.6	77.2 ± 13.6	24.8 ± 1.1
PU-PCL	20.5 ± 0.4	169.5 ± 14.1	69.3 ± 0.6
PU-PCL/PCM1	19 ± 0.5	178.3 ± 11.5	43.3 ± 1.6
PU-PCL/PCM2	17.1 ± 0.7	221.4 ± 23.7	41.2 ± 0.8